

Determination of the Wavelength Dependence of Refractive Indices of Flame Soot

H. Chang and T. T. Charalampopoulos

Proc. R. Soc. Lond. A 1990 **430**, 577-591

doi: 10.1098/rspa.1990.0107

References

Article cited in:

<http://rspa.royalsocietypublishing.org/content/430/1880/577#related-urls>

Email alerting service

Receive free email alerts when new articles cite this article - sign up in the box at the top right-hand corner of the article or click [here](#)

Determination of the wavelength dependence of refractive indices of flame soot

BY H. CHANG AND T. T. CHARALAMPOPOULOS

*Department of Mechanical Engineering, Louisiana State University,
Baton Rouge, Louisiana 70803, U.S.A.*

The spectral variation of the optical properties of soot particles is determined by combining classical and dynamic light scattering measurements with the Kramers–Krönig relations. Particle size and number densities are determined from scattering/extinction and autocorrelation measurements at the wavelength of 0.488 μm . This information is then combined with the spectral extinction measurements in the wavelength range 0.2 to 6.4 μm to determine the spectral variation of the refractive indices of flame soot. Results are presented for a premixed propane–oxygen flame with a fuel equivalence ratio $\phi = 1.8$. The sensitivity of the technique and its advantage over the previous methods are discussed.

1. Introduction

Knowledge of the wavelength dependence of the optical properties of soot over the entire spectrum is important for radiative transfer calculations. In addition, laser-based techniques for *in situ* oxidation and growth studies require accurate refractive indices at specific wavelengths. Several investigators have dealt with the wavelength dependence of the refractive index of soots both theoretically and experimentally. Stull & Plass (1960) derived a set of dispersion equations for the calculation of the optical properties of carbon at flame temperatures. Foster & Howarth (1983) measured the reflection of plane polarized light from compressed soot specimens in the wavelength range 1–10 μm . The refractive indices were then inferred from the ratio of the intensities in both planes of polarization in three angles of incidence 60°, 70° and 80° of greater accuracy. Dalzell & Sarofim (1969) measured the reflection coefficients from soot pellet surfaces at 30° from the normal in the wavelength range 0.40–10 μm and inverted the data using the Fresnel equations. The inferred index spectra were combined with the multivariable Drude–Lorentz dispersion model to provide values for the dispersion constants. Lee & Tien (1981) utilized *in situ* transmission data of plexiglass and polystyrene flames to determine a more rigorous set of dispersion constants. Tomaselli *et al.* (1981) used the reflection coefficients of compressed soot (Mogul L carbon black) to determine the optical constants in the 3–14 μm region. The reflection technique was also used by Felske *et al.* (1984) to determine the refractive indices of soot generated in a propane diffusion flame in the wavelength range 2–10 μm . In that study, it was also demonstrated that the reflection technique can yield the refractive indices of soot in the infrared region provided that the pellet surfaces possess high specular index and that the data are corrected for voidage effects. Batten (1985) determined the optical constants of

Proc. R. Soc. Lond. A (1990) **430**, 577–591 Printed in Great Britain

carbonaceous materials derived from various types of fuels using a polarization ratio reflectance technique over the spectral range 0.50–0.75 μm . More recently, a technique was developed by Charalampopoulos & Felske (1987) which can yield the refractive index of soot under flame conditions by combining scattering/extinction and dynamic light scattering measurements with the ratio of the real and imaginary part of the complex electrical permittivity. In a more recent study Charalampopoulos & Chang (1988) applied the same technique in a premixed propane–oxygen flame to determine the refractive indices in the visible wavelengths 0.458–0.514 μm . A set of dispersion constants was also presented by combining the spectral extinction measurements in the visible wavelengths 0.30–0.65 μm and the known particle number density and particle size distribution with the Drude–Lorentz dispersion model. Habib & Vervisch (1988) also used spectral extinction data from premixed methane, propane and ethylene flames in conjunction with the dispersion model and proposed a different set of dispersion constants.

Despite the available data for the spectral variation of the indices based on the estimated values of the dispersion constants there exists a significant uncertainty as to their actual values. The uncertainty is due both to the questionable validity of the dispersion model for representing the actual behaviour of the soot refractive indices and to the limited number of unknowns that can be extracted from a set of transmission data (see, for example, Latimer 1972; Janzen 1979, 1980). In addition, as it has been pointed out by Menna & D'Alessio (1982) the existing dispersion models for soot do not predict correctly the *in situ* spectral scattering/extinction measurements in the ultraviolet part of the spectrum. On the other hand, the reflection technique, although useful in the infrared wavelengths when the voidage effects are accounted for (see Felske *et al.* 1984) may yield inaccurate results when the temperature variation is neglected (see Howarth *et al.* 1966; Charalampopoulos *et al.* 1989). The present study uses spectral extinction measurements in the wavelength range 0.20–6.4 μm in combination with the Kramers–Krönig relations to determine the refractive indices of flame soot over the whole spectrum. The photon correlation method was used in the autocorrelation mode to determine the particle size distribution. The particle number density was determined by combining the scattering/extinction measurements in the wavelength 0.488 μm with the ratio of the real and imaginary part of the complex electrical permittivity (see Charalampopoulos & Chang 1988). To illustrate the approach results are presented for a premixed propane–oxygen flame with fuel equivalence ratio of $\phi = 1.8$ in the wavelength range 0.20–30 μm . In addition, to facilitate calculations of the indices relations are presented that yield accurate values in the wavelength region 0.40–30 μm . The advantages and shortcomings of the method with respect to the previous techniques as well as its sensitivity are assessed.

2. Theory

The Kramers–Krönig (KK) relations have been applied in the analysis of reflectance data from graphite by Taft & Philipp (1965) and by Goodwin & Mitchner (1984) in studying the near infrared optical constants of coal ash. The KK relations are derived from the principles of causality and require a linear relation between the input and output of a passive physical system (see, for example, Newton 1966; Nussenzweig 1972; Bohren & Huffman 1983).

Let the response of such a system be represented by the complex function $A(\omega) = A_r(\omega) - iA_i(\omega)$. Then, the KK relations imply that the real and imaginary part of the function may be expressed as

$$A_r(\omega) = \frac{2}{\pi} \text{P} \int_0^\infty \frac{\omega' A_i(\omega')}{\omega'^2 - \omega^2} d\omega', \quad (1)$$

and

$$A_i(\omega) = -\frac{2}{\pi} \text{P} \int_0^\infty \frac{\omega A_r(\omega')}{\omega'^2 - \omega^2} d\omega', \quad (2)$$

where P indicates the Cauchy principal value of the integral and ω is the angular frequency of the radiation.

For a spherical soot particle of radius r the scattering amplitude function S_0 in the forward direction (see Ku & Felske 1986) satisfies the KK relations

$$\begin{aligned} A(\omega) &= A_r(\omega) - iA_i(\omega) \\ &= -i[\text{Re}(S_0) - i \text{Im}(S_0)]/x^3, \end{aligned} \quad (3)$$

where Re and Im signify the real and imaginary part of the complex function S_0 , and x represents the size parameter ($x = 2\pi r/\lambda$) at the wavelength λ of the incident radiation. The function S_0 is given by the Mie theory (1908) and depends on the particle refractive index and size parameter. Furthermore, from the optical theorem (see Bohren & Huffman 1983) the extinction efficiency Q_e of a spherical particle is related to the complex scattering function S_0 and consequently the imaginary part of $A(\omega)$ may be expressed as

$$\begin{aligned} Q_e &= 4 \text{Re}(S_0)/x^2 \\ &= 4x A_i(\omega). \end{aligned} \quad (4)$$

In sooting flames, such as the flame used in this study, a distribution of particle sizes exists and therefore the measured spectral transmittance τ_λ through the homogeneous pathlength L may be written as

$$\tau_\lambda = \exp \left[- \int_0^\infty \pi r^2 Q_e NLP(r) dr \right], \quad (5)$$

where N is the particle number density (cm^{-3}) and $P(r)$ is the zeroth-order lognormal distribution (ZOLD) function (see Kerker 1969) given by

$$P(r) = \frac{\exp(-\ln^2 \sigma/2)}{\sqrt{2\pi} r_0 \ln \sigma} \exp \left[-\frac{\ln^2(r/r_0)}{2 \ln^2 \sigma} \right]. \quad (6)$$

The parameters r_0 and σ represent the average radius and the geometric width of the distribution and are determined from photon correlation measurements. It is noted that the zeroth-order lognormal distribution function was selected based on the results of previous studies. Specifically, as it has been noted by Wersborg *et al.* (1973) and Prado *et al.* (1981) the size distribution of soot in flames similar to the one used in the present study progresses from being mainly gaussian in the early stages of particle formation to mainly lognormal in the later stages. Furthermore, previous studies of soot size distribution in premixed flames using photon correlation (see Charalampopoulos & Chang 1988; Charalampopoulos *et al.* 1989) utilized the zeroth-order lognormal distribution function. Combining equations (4) and (5) yields:

$$\tau_\lambda = \exp \left[\frac{-8\pi^2 NL}{\lambda} \int_0^\infty r^3 A_i(\omega) P(r) dr \right]. \quad (7)$$

This equation can be expressed in a more useful form by introducing the volume weighted mean radius r_m defined as

$$r_m = \left[\int_0^\infty r^3 P(r) dr \right]^{1/3}, \quad (8)$$

which after integration yields

$$r_m = r_0 \exp(2.5 \ln^2 \sigma). \quad (9)$$

With this definition, the complex part of the function $A(\omega)$ for the polydisperse distribution of particles may be expressed as

$$\bar{A}_i(\omega) = \int_0^\infty \left(\frac{r}{r_m} \right)^3 A_i(\omega) P(r) dr, \quad (10)$$

which when substituted into equation (7) yields for the spectral transmittance

$$\tau_\lambda = \exp[-8\pi^2 r_0^3 \exp(7.5 \ln^2 \sigma) NL \bar{A}_i(\omega) / \lambda]. \quad (11)$$

Thus by inferring the parameters (r_0, σ) from the photon correlation measurements the function $\bar{A}_i(\omega)$ may be computed from the measured spectral transmittance τ_λ at each wavelength λ using equation (11). It is noted that although the function $A_r(\omega)$ may be evaluated from equation (1) a more useful expression may be obtained using the subtractive Kramers–Krönig (SKK) technique (Ahrenkiel 1971). This technique is less sensitive to extrapolation beyond the range of the available experimental data and possesses better convergence. The SKK relation for $A_r(\omega)$ is obtained by first evaluating equation (1) at $\omega = 0$ and then subtracting the result from equation (1). Therefore, the function $A_r(\omega)$ for the polydisperse system of particles takes the form

$$\bar{A}_r(\omega) = 1 + \frac{2\omega^2}{\pi} P \int_0^\infty \frac{\bar{A}_i(\omega')}{\omega'(\omega'^2 - \omega^2)} d\omega'. \quad (12)$$

Since the function $\bar{A}_i(\omega')$ can be obtained experimentally over a finite range of wavelengths ($0.2 \leq \lambda \leq 6.4 \mu\text{m}$ in this study) extrapolation expressions for $\bar{A}_i(\omega)$ were developed to carry out the full integration according to equation (12). The extrapolation relations are discussed in the next section. With the functions $\bar{A}_i(\omega)$ and $\bar{A}_r(\omega)$ determined the left-hand side of equations (3) is completely defined, and for the polydisperse system of particles it follows that

$$\bar{A}_i(\omega) = \exp(-7.5 \ln^2 \sigma) \frac{1}{x_0^3} \int_0^\infty \text{Re}(S_0) P(r) dr, \quad (13)$$

and

$$\bar{A}_r(\omega) = -\exp(-7.5 \ln^2 \sigma) \frac{1}{x_0^3} \int_0^\infty \text{Im}(S_0) P(r) dr, \quad (14)$$

where $x_0 = 2\pi r_0 / \lambda$ and the integration is over all possible radii. For monodisperse system of particles ($\sigma = 1$) equations (13) and (14) reduce to

$$\bar{A}_i(\omega) = A_i(\omega) = \text{Re}(S_0) / x^3, \quad (15)$$

and

$$\bar{A}_r(\omega) = A_r(\omega) = -\text{Im}(S_0) / x^3. \quad (16)$$

Consequently, the refractive indices (n, k) may be determined at each wavelength λ by simultaneously solving equations (13) and (14) for the polydisperse system and

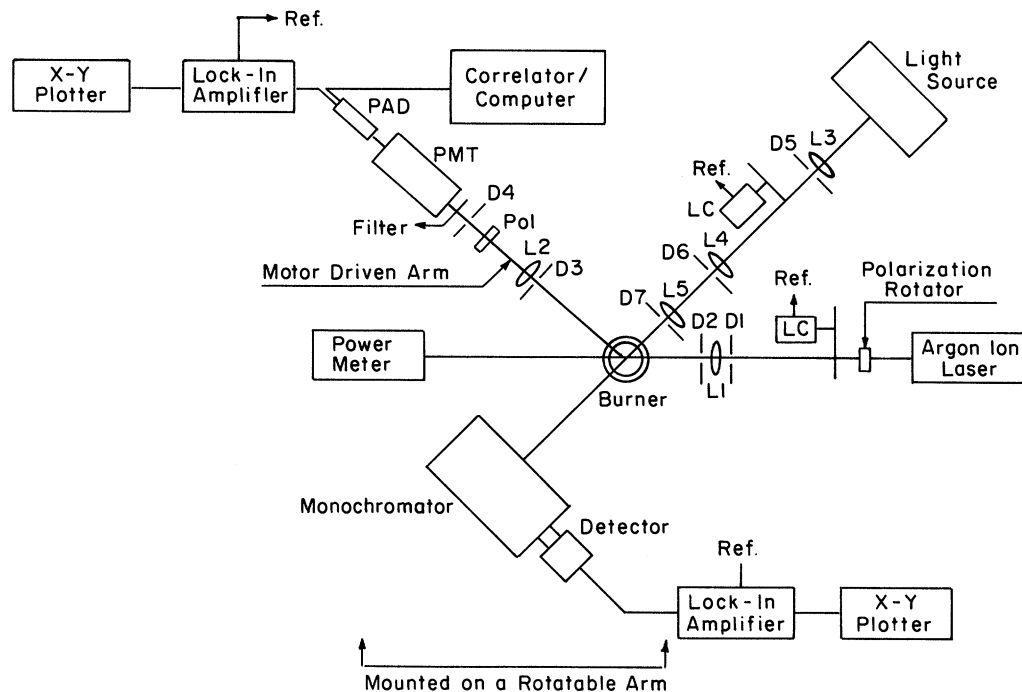


Figure 1. Plan view of the light scattering system.

equations (15) and (16) for the monodisperse system of particles. In the present study the data were analysed both for the monodisperse and polydisperse systems. However, due to the insignificant differences only the polydisperse system results will be presented. The method of data analysis as well as the experimental technique along with the results and discussion for a premixed propane–oxygen flame at a fuel equivalence ratio $\phi = 1.8$ are presented in the following sections.

3. Data analysis

The main difficulty associated with the data inversion using the **KK** relations is that experimental data can only be obtained for a limited range of wavelengths. However, as it may be seen from equation (1) measurements are needed over all wavelengths. In this study the **SKK** technique was used since it is less sensitive to the extrapolation beyond the wavelengths of experimental range. To test the **KK** method of analysis computations were carried out in the frequency range 0.005 to 30 eV ($0.04 \leq \lambda \leq 248 \mu\text{m}$). The required refractive indices (for the computation of Q_e) were generated from the dispersion constants obtained from spectral extinction measurements in a premixed propane–oxygen flame with fuel equivalence ratio $\phi = 1.8$. The function $A_1(\omega)$ was then obtained in the range $0.2 \leq \lambda \leq 27 \mu\text{m}$ and with particle radii typical of flame soot $0.01 \leq r \leq 0.10 \mu\text{m}$. For the wavelength range above and below the upper (ω_n) and lower (ω_1) limits of integration analytical expressions were developed. Several functional forms were tried. However, the expressions that provided the best agreement are the following:

$$A_1(\omega) = (b/\omega) (x^{-1} + x^{-2} + x^{-3} + x^{-4}), \quad (17)$$

for the wavelength range 0.04 to 0.2 μm and

$$A_i(\omega) = c_1 \omega + c_2 \omega^2 + c_3 \omega^3 + c_4 \omega^4, \quad (18)$$

for the range 27 to 248 μm . It is noted that for large wavelengths, as it may be seen from figures 2 and 3, the functions \bar{A}_i and \bar{A}_r do not depend on the size distribution parameters (r_0, σ). This is because for large wavelengths most of the particles in the distribution behave as Rayleigh scatterers and in the Rayleigh limit \bar{A}_i and \bar{A}_r are not functions of the size distribution parameters. The constant b is computed from the measured value of $A_i(\omega_h)$ and the constants c_i ($i = 1, 2, 3, 4$) are computed from measured values of A_i at ω_1 and three other frequencies near ω_1 . On the other hand, for small wavelengths, it can be seen that both functions \bar{A}_i and \bar{A}_r are very sensitive to the values of the size distribution parameters (r_0, σ). Specifically, when the particle radius changes by a factor of ten the value of the function changes by a factor of two. Thus, special attention is required to obtain the average particle radius and the geometric width σ with the maximum possible accuracy from the photon correlation measurements. The refractive indices n and k were then reproduced using the KK method of analysis to within 2.5% from those predicted by the dispersion models in the wavelength range $0.25 \leq \lambda \leq 25 \mu\text{m}$. The calculations demonstrated that the inferred refractive index spectra are insensitive to the extrapolations of the function A_i in the region of long wavelengths. Specifically it was found that transmission measurements in the range of wavelengths $0.2 \leq \lambda \leq 6.4 \mu\text{m}$ should be sufficient to infer reliable indices.

4. Experimental measurements

The experimental set up for the scattering/extinction and photon correlation measurements at the single wavelength of 0.488 μm and of the spectral extinction coefficients in the wavelength range 0.2 to 6.4 μm is shown in figure 1. All measurements were performed in a premixed propane–oxygen flame with fuel equivalence ratio $\phi = 1.8$ and unburned gas velocity 1.75 cm s^{-1} . The flame was surrounded by a shroud of nitrogen with velocity of 5.6 cm s^{-1} and supported by a Corning honeycomb made of cordiorite with 31 cells per square centimetre, 144 mm in diameter and 76 mm long. A vertically polarized 3 W Argon ion laser was used for the single wavelength scattering/extinction measurements. The spectral extinction coefficients were measured using a 150 W xenon lamp and an infrared glowing resistor. The light beams in both cases were chopped at 600 Hz and focused onto the central axis of the burner by the system of lenses (L1 and L3–L5). The scattered light from the laser was detected at 90° with a photomultiplier tube model 9863B/350 EMI. The scattering coefficients of the soot particles in the vertical–vertical polarization orientation at 90° ($\sigma_{vv}, 90^\circ, \text{cm}^{-1} \text{str}^{-1}$) were determined by measuring the scattered flux from a stream of high purity methane gas flowing through the burner. The settings for the optical and electronic components were identical with those used for the measurement of the scattered fluxes from the sooting flame. The scattered fluxes in both cases were corrected for the attenuation between the scattering volume and the detector. The parameters of the particle size distribution (r_0, σ) were determined using the photon correlation technique. To minimize the experimental uncertainties the same detector and detection optics was used for the autocorrelation measurements at an angle 7° from the forward direction. The flame temperatures required for the determination of the particle size distribution using

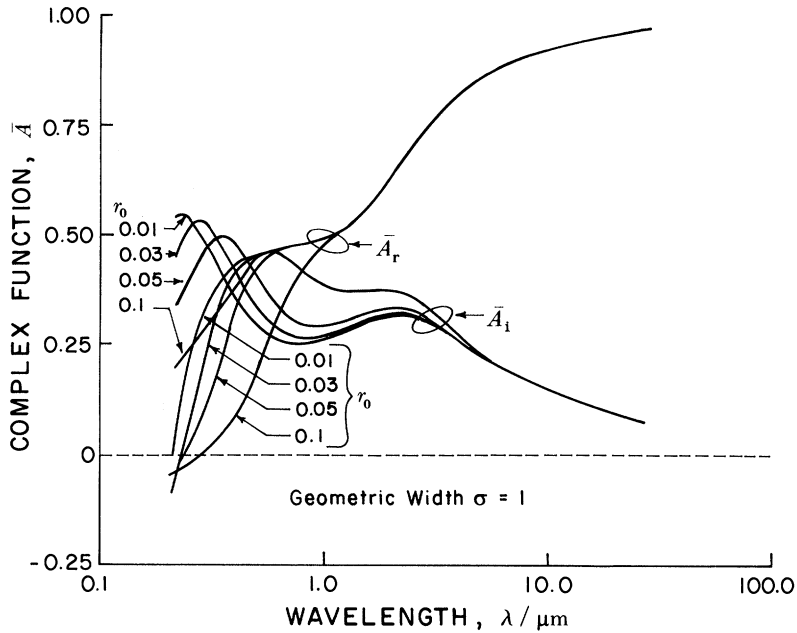


Figure 2. Variation of the functions \bar{A}_1 and \bar{A}_r with respect to the wavelength for particle radii in the range 0.01 to 0.1 μm .

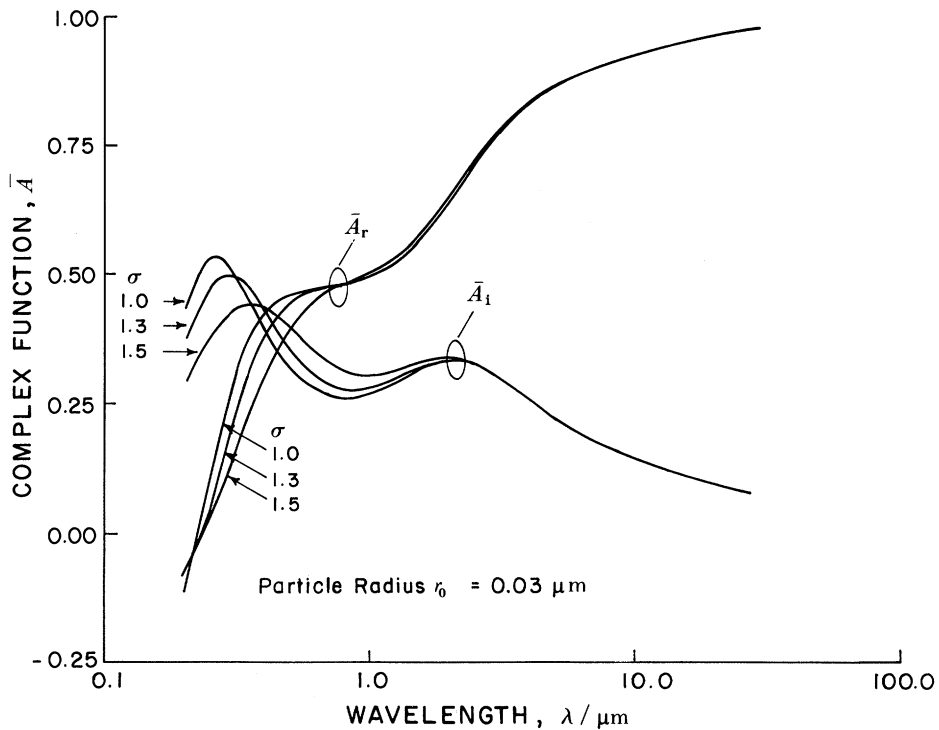


Figure 3. Variation of the functions \bar{A}_1 and \bar{A}_r with respect to geometric width (σ) and wavelength (λ). The particle radius used was 0.03 μm .

Table 1. *Light sources, detectors and wavelength range for monochromator gratings and long pass filters used for the spectral extinction coefficients*

light source ...	xenon		silicon carbide glowbar			
detector	1P28 (RCA)	InSb (SBRC)		InSb		HgCdTe
wavelength range/ μm	0.2–0.6	0.6–1.1	1.1–1.8	1.8–3	3–5	5–7
gratings						
wavelength region/ μm	0.18–0.7	0.6–2	0.6–2	1.2–4	2.4–8	4.8–16
filters						
5% cut-on wavelength	0.3	0.55	0.95	1.5	2.5	4.5

Table 2. *Temperature (T), particle radius (r_0), geometric width (σ), number density (N), scattering coefficients (σ_{vv} , 90° , $\text{cm}^{-1} \text{str}^{-1}$) and extinction coefficient (K_{ext} , cm^{-1}) at the wavelength $0.488 \mu\text{m}$ as a function of position above the burner surface (H)*

H/mm	T/K	r_0/nm	σ	$N \times 10^{-9}$ cm^{-3}	$\sigma_{\text{vv}} \times 10^4$ $\text{cm}^{-1} \text{sr}^{-1}$	$K_{\text{ext}} \times 10^2$ cm^{-1}
6	1330	19.1	1.215	12.2	1.0	5.7
7	1285	21.8	1.207	9.6	1.6	6.7
8	1250	23.7	1.212	8.4	2.6	7.9
9	1225	25.7	1.209	7.1	3.7	8.7
10	1195	27.5	1.200	6.4	4.8	9.6
12	1150	30.0	1.211	5.2	7.3	10.7
14	1130	32.7	1.204	4.3	9.0	11.5
16	1100	34.1	1.213	4.0	10.8	12.3

the photon correlation measurements were carried out with a Pt–Pt/13% Rd thermocouple. The required transmission measurement at the single wavelength of $0.488 \mu\text{m}$ was carried out in two different ways. In the first case the transmission was measured by a power laser meter model 404 Spectra Physics. In the second case the transmission at the same wavelength was measured by a 150 W xenon lamp. The beam from the xenon lamp was dispersed by a grating monochromator, ORIEL model 77250 (see table 1). The transmitted intensities were detected by an RCA 1P28 photomultiplier tube in the ultraviolet and visible wavelengths. Indium antimonide (InSb) and mercury cadmium telluride (HgCdTe) detectors were used for the infrared wavelengths. The system for the spectral extinction measurements was calibrated using the emission lines of a mercury arc lamp and the absorption of polystyrene film and liquid chloroform. The reference intensities (without flame) were measured before and after each measurement, at each wavelength, to ensure that the light intensity remains unchanged throughout the experiment. More details about the experimental facility, the measurement technique, and the determination of the number densities from *in situ* single wavelength scattering/extinction measurements have been reported previously (Charalampopoulos 1987).

5. Results

The particle radii, geometric width σ and the scattering/extinction coefficients along with the flame temperature (T) as a function of position above the burner surface are shown in table 2. The magnitudes and trends of the measured quantities are consistent with previous investigations. Measured spectral extinction coefficients

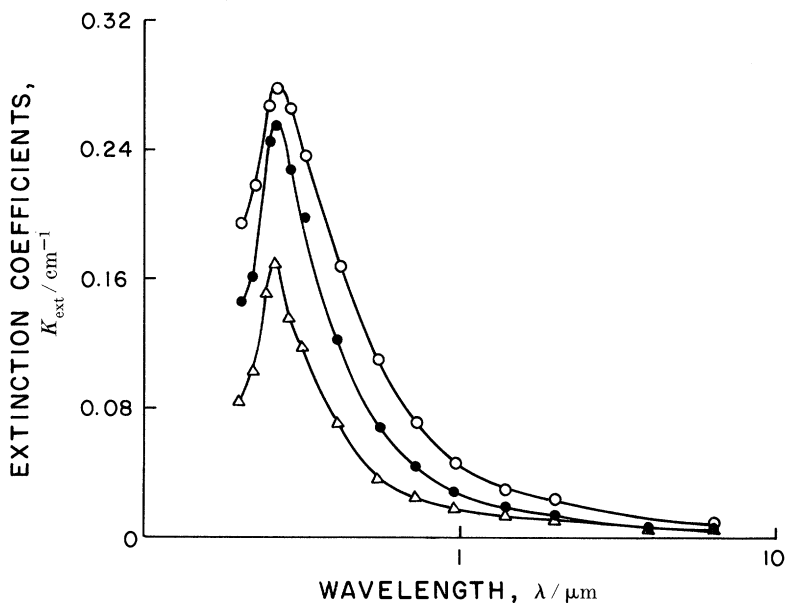


Figure 4. Measured spectral extinction coefficients for the premixed propane–oxygen flame with $\phi = 1.8$. H (mm): Δ , 6; \bullet , 10; \circ , 16.

for the propane–oxygen flame are shown in figure 4 for three different positions (H) above the burner surface. A marked maximum of extinction coefficient is observed in the ultraviolet region 0.25–0.26 μm . The maxima are shifted towards longer wavelengths as the height above the burner surface increases. This behaviour is consistent with the results reported by Menna & D’Alessio (1982), who found that the peaks occur in the wavelength region 0.23–0.250 μm . Although a satisfactory explanation is not possible at this time, the difference may be attributed to the fact that different flames were investigated in the two studies. This might have resulted in particles with slightly different chemical compositions and thus different absorption characteristics. The spectra of the real and imaginary part of the index determined from the Kramers–Krönig analysis are shown in figure 5. Predictions of the index spectra by the dispersion models proposed by Dalzell & Sarofim (1969) and Lee & Tien (1981) are also shown. As it may be seen these models predict a monotonic decrease for the real part of the index in the ultraviolet. The results of the present study show a behaviour which is similar to the resonance of the glassy carbon and corresponds probably to π band transitions as in the case of graphite (see, for example, Taft & Philipp 1965; Haering & Mrozowski 1960). It should be noted that electron microscopy and X-ray diffraction studies (see Lahaye & Prado 1981) show that soot particles consist of turbostratic graphitic layers, randomly oriented and connected to one another by amorphous carbon.

For convenience, values of the inferred indices as a function of the wavelength and position above the burner surface are shown in table 3. In addition, to facilitate calculations of the indices, at any wavelength, expressions are provided for the real and imaginary part of the index that are valid for the wavelength range $0.4 \leq \lambda \leq 30 \mu\text{m}$. The most accurate expressions are of the form:

$$n = 1.811 + 0.1263 \ln \lambda + 0.027 \ln^2 \lambda + 0.0417 \ln^3 \lambda, \quad (19a)$$

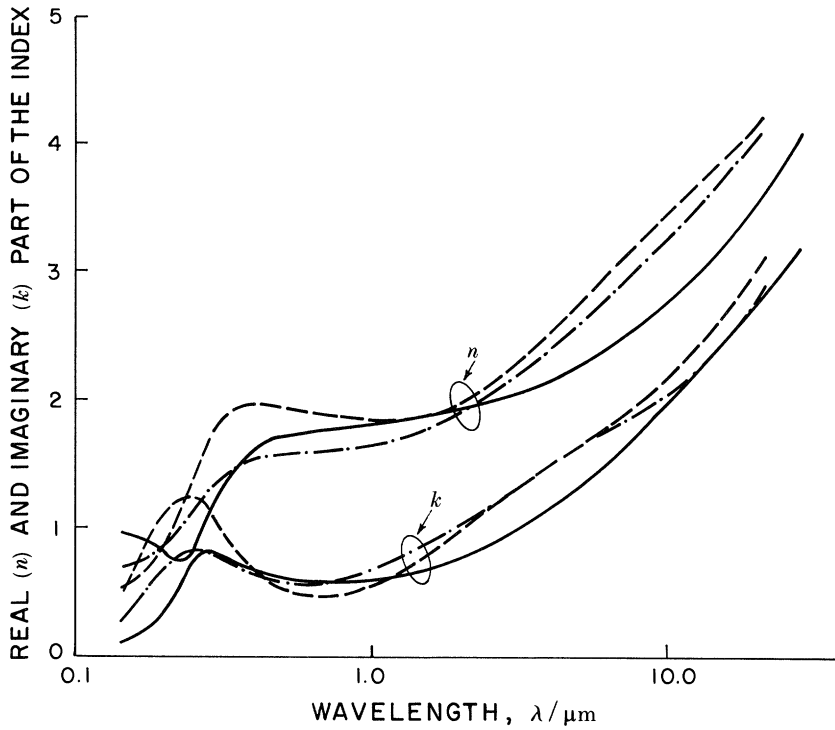


Figure 5. Comparison of spectral refractive index determined in the present study using Kramers–Krönig analysis with other studies. —, This work; ---, Lee & Tien (1981); -·-·-, Dalzell & Sarofim (1969).

Table 3. *Optical properties of propane flame soot with fuel equivalence ratio $\phi = 1.8$ as a function of the wavelength and position above the burner surface (H)*

$\lambda/\mu\text{m}$	height above the burner surface, H/mm					
	6		8		10	
	n	k	n	k	n	k
0.20	0.78	0.32	0.82	0.40	0.94	0.35
0.26	1.04	0.78	0.97	0.81	1.19	0.79
0.40	1.50	0.65	1.60	0.66	1.64	0.67
0.54	1.63	0.48	1.73	0.58	1.77	0.63
0.71	1.61	0.47	1.76	0.56	1.82	0.57
1.00	1.65	0.50	1.82	0.54	1.92	0.56
2.16	1.83	0.75	1.95	0.80	2.03	0.81
3.89	2.10	1.11	2.18	1.11	2.25	1.18
6.24	2.33	1.41	2.39	1.45	2.47	1.52
10.9	2.78	1.87	2.84	2.02	2.96	2.10
16.8	3.20	2.34	3.35	2.53	3.47	2.60
21.1	3.47	2.58	3.64	2.83	3.79	2.98
28.4	3.87	3.00	4.09	3.27	4.26	3.37

Table 4. Percentage differences between values of the indices determined from the Kramers–Krönig analysis and those calculated from the approximate relations (19) as a function of the wavelength (λ) and the height above the burner surface (H)

H/mm	6		8		10	
	n	k	n	k	n	k
0.4	9.8	3.4	5.6	2.9	3.2	1.5
0.54	5.9	14.7	0.5	3.5	2.9	4.2
0.71	9.2	11.9	0.4	5.2	4.9	0.1
1.0	7.5	13.9	2.0	6.4	6.6	0.9
3.89	1.7	3.2	1.8	0.5	5.3	3.4
6.24	2.7	7.0	0	2.9	3.3	3.4
10.9	2.5	7.0	0.3	1.4	4.1	3.3
16.8	3.6	7.5	1.2	0	4.3	3.8
21.1	4.7	7.9	1.0	1.1	4.2	4.9
28.4	5.6	5.6	0.8	2.9	3.8	5.6

for the real part and

$$k = 0.5821 + 0.1213 \ln \lambda + 0.2309 \ln^2 \lambda - 0.01 \ln^3 \lambda, \quad (19b)$$

for the imaginary part. These expressions provide indices that agree, on the average, to within 5% for n and 6% for k with the values obtained from the Kramers–Krönig analysis at the height of 8 mm above the burner surface. The same expressions may be used for the heights of 6 and 10 mm above the burner surface. The percentage differences between the inferred indices from the Kramers–Krönig analysis and the above expressions in the wavelength range 0.40–28.4 μm for all three heights above the burner surface are presented in table 4.

It should be noted that the accuracy of the inferred indices depends on the levels of the uncertainty associated with the particle diameter, the scattering/extinction coefficient at the single wavelength as well as on the accuracy of the spectral extinction coefficients. The sensitivity of the particle radius to the measured temperature is insignificant due to the weak dependence of the particle diffusion on temperature (see, for example, Charalampopoulos & Felske 1987). On the other hand, the uncertainty in the inferred number density depends strongly on the particle radius. This is because when the scattering or absorption measurements are used to solve for the number density a dependence on the sixth or third power of the particle radius arises. Thus, to obtain the particle number density that is needed in the data inversion with minimum uncertainty, the scattering/extinction coefficients and the particle radius must be determined with the maximum possible accuracy. It is noted that in the present study the data analysis was carried out both for monodisperse and polydisperse system of particles. As it should have been expected the inferred index spectra in both cases agree very well. Specifically, the percent difference for the real part of the index in the wavelength range 0.20–25 μm between the monodisperse and polydisperse results is 1.8% whereas the corresponding difference for k is 1.3%. In the KK method of analysis the function $\bar{A}_i(\omega)$ is first computed from the measured transmittance and the index spectra are determined by solving simultaneously equations (13) and (14) at each wavelength. Thus, the uncertainty in n and k will depend on the fluctuation of the functions $\bar{A}_i(\omega)$ and $\bar{A}_r(\omega)$ from their actual values. It should be noted that the logarithmic nature of the measured transmittance requires that extreme care should be exercised in obtaining the extinction

Table 5. *Combined root mean square values in the inferred index spectra*

wavelength/ μm		0.54	1.0	6.24	10.9	16.8	21.1	28.4
combined r.m.s.	<i>n</i>	11	12	13	13	14	14	16
	<i>k</i>	4	15	14	13	14	14	15

measurements. Towards this end multiple sets of transmittance measurements were carried out and only the data that possessed the minimum possible fluctuation above and below the average values were utilized in the data inversion. To assess the uncertainty in the inferred index spectra a $\pm 0.5\%$ fluctuation in the used average transmittance values and $\pm 5\%$ in the particle radius and particle number density were assumed. The total uncertainty for the reported index spectra based on the parameters utilized for the data inversion in this study is summarized in table 5. Further discussion on additional factors influencing the inferred index spectra are presented in the following section.

6. Discussion

As it was mentioned earlier apart from the error introduced because of the extrapolation associated with the Kramers–Krönig relations several other factors may contribute to the uncertainties of the refractive index of the particle as it exists under flame conditions. It should be noted that reliable data analysis is only possible for positions in the flame where the ‘diffusional’ diameter measured by the photon correlation can be considered to be the same with the ‘optical’ diameter as required by the Mie equations. This limits the region in the flame where data analysis can yield the soot indices with the minimum possible uncertainty. Furthermore, as it has been noted by several investigators (see, for example, Haynes & Wagner 1980; D’Alessio 1981; Weiner & Harris 1989) the measured extinction in these type of flames is the sum of the contributions from the molecular species such as polycyclic aromatic hydrocarbons (PAH) as well as soot particles. Haynes & Wagner have shown that absorption occurs early in a premixed benzene–air flame and estimated the gas-phase absorption profiles in the wavelength range 0.366–0.808 μm on the assumption that the extinction at 0.808 μm is due solely to soot. On the other hand, D’Alessio (1981) attributed the observed ultraviolet absorption peaks entirely to molecular absorbers. However, it has been pointed out by Menna & D’Alessio (1982) that the soot contribution to the total measured extinction may not be computed accurately using the available dispersion models in the ultraviolet. This is because the existing dispersion models do not account for the resonant behaviour of the optical properties in this part of the spectrum. Recently, Weiner & Harris (1989) reported molecular absorbance data in the visible wavelengths obtained by subtracting the absorbance due to soot particles. As they pointed out, the results of the subtraction depend strongly on the values used for the refractive index. Similar calculations carried out in this study corroborate this observation. Thus, knowledge of the absorption and scattering coefficients corresponding to all species other than the soot particles is needed to determine the ‘absolute’ scattering and absorption coefficients of soot. In the present study, as a first step, towards accounting for the gaseous absorption contribution to the total extinction the percent absorption for a non-sooting propane–oxygen flame was measured at three different heights in the flame. The measured absorption spectra (see figure 6) are consistent with previous works (see

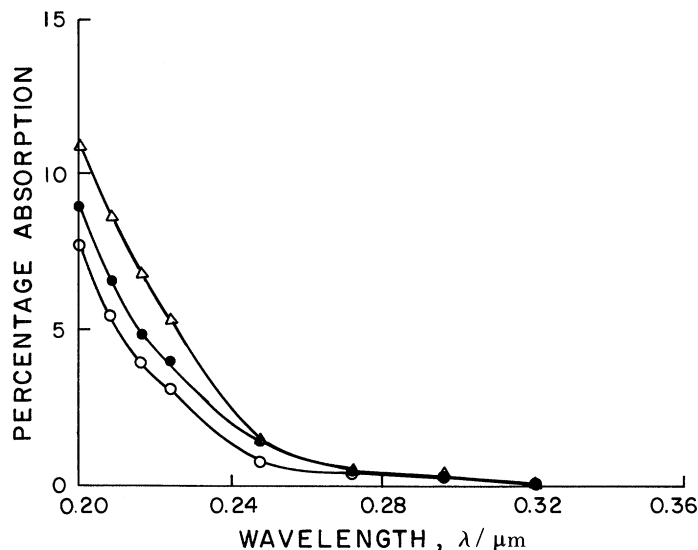


Figure 6. Percentage absorption measurements for a non-sooting propane–oxygen flame from 0.2 to 0.35 μm . H (mm): Δ , 6; \bullet , 12; \circ , 16.

Di Lorenzo *et al.* 1981) both in terms of wavelength and position above the burner surface. It is noted that the contribution of the gaseous absorption to the total extinction becomes more pronounced at the ultraviolet wavelengths. Specifically at 0.20 and 0.26 μm the gaseous absorption to the total extinction corresponds to 29% and 2% respectively, at the height of 6 mm above the burner surface. This results in an increase in the real and imaginary part of the index by 4.0% and 4.8% respectively at 0.26 μm . It should also be pointed out that the single particle assumption and subsequent analysis using the Mie theory can be called into question. This is because of the agglomeration of the primary particles into clusters, as well as random and straight chains. The prediction of the scattering/extinction cross section for agglomerates consisting of primary particles with size parameters in the Rayleigh régime can be accomplished using the theory developed by Jones (1979). A sensitivity analysis was carried out in a previous study for agglomerates with number of primary particles less than thirty (Charalampopoulos & Chang 1988) and it was concluded that the difference in the index of the primary particle and that of the agglomerate was indeed small. For the position in the flame for which data are presented in this study it is reasonable to expect that the degree of agglomeration is limited. Nevertheless, the inferred indices can only be considered as ‘effective’ and not ‘absolute’. However, it should be pointed out that the present method can yield the ‘effective’ refractive indices over the whole spectrum with the least number of assumptions as compared with the Drude–Lorentz dispersion model that has been used so far. The main limitations of the approach are that (1) accurate infrared transmission measurements under flame conditions are difficult to obtain and (2) the experimental uncertainty over the whole range of measurements and especially in the infrared upper limit must be as low as possible.

7. Conclusion

The spectral variation of the refractive index of soot particles has been determined by combining classical and dynamic light scattering measurements with the Kramers–Krönig relations. The optical properties exhibit a resonance in the ultraviolet which resembles glassy carbon data in band structure. It was also shown that the present method could yield the refractive index of soot over the whole spectrum with the least number of assumptions as compared with previous methods.

This research was supported in part by the National Science Foundation through grant CBT-882-480.

References

- Ahrenkiel, R. K. 1971 Modified Kramers–Krönig analysis of optical spectra. *J. opt. Soc. Am.* **61**, 1652.
- Batten, C. E. 1985 Spectral optical constants of soots from polarized angular reflectance measurements. *Appl. Optics* **24**, 1193.
- Bohren, C. F. & Huffman, D. R. 1983 *Absorption and scattering of light by small particles*. New York: Wiley-Interscience.
- Charalampopoulos, T. T. 1987 Automated light scattering system and a method for the in-situ measurement of the index of refraction of soot particles. *Rev. Sci. Inst.* **58**, 1638.
- Charalampopoulos, T. T. & Chang, H. 1988 *In situ* optical properties of soot particles in the wavelength range from 340 to 600 nm. *Comb. Sci. Tech.* **59**, 401.
- Charalampopoulos, T. T. & Felske, J. D. 1987 Refractive indices of soot particles deduced from in situ laser light scattering measurements. *Comb. Flame* **68**, 283.
- Charalampopoulos, T. T., Chang, H. & Stagg, B. 1989 The effect of temperature and composition on the complex refractive index of flame soot. *Fuel* **68**, 1173.
- D'Alessio, A. 1981 Laser light scattering and fluorescence diagnostics in rich flames produced by gaseous and liquid fuels. *Particulate carbon* (ed. D. C. Siegla & G. W. Smith). New York: Plenum Press.
- Dalzell, W. H. & Sarofim, A. F. 1969 Optical constants of soot and their applications to heat flux calculations. *J. Heat Transfer* **91**, 100.
- Di Lorenzo, A., D'Alessio, A., Cincotti, V., Masi, S., Menna, P. & Venitozzi, C. 1981 UV absorption, laser excited fluorescence and direct sampling in the study of the formation of polycyclic aromatic hydrocarbons in rich CH₄/O₂ flames. *Eighteenth Symp. (Int.) on Combustion*, p. 485. The Combustion Institute.
- Felske, J. D., Charalampopoulos, T. T. & Hura, H. 1984 Determination of the refractive indices of soot particles from the reflectivities of compressed soot pellets. *Comb. Sci. Tech.* **37**, 263.
- Foster, P. J. & Howarth, C. R. 1963 Optical constants of carbon and coals in the infrared. *Carbon* **6**, 719.
- Goodwin, D. G. & Mitchner, M. 1984 Measurements of the near infrared optical properties of coal ash. *ASME Heat Transfer Conf.* 84-HT-41.
- Habib, Z. G. & Vervisch, P. 1988 On the refractive index of flame soot at flame temperature. *Comb. Sci. Tech.* **59**, 261.
- Haering, R. R. & Mrozowski, S. 1960 The band structure and electronic properties of graphite crystals. *Proc. in Semiconductors*, 5, p. 273. New York: Wiley-Interscience.
- Haynes, H. & Wagner, H. G. 1980 Optical studies of soot formation processes in premixed flames. *Ber. Bunsenges. Phys. Chem.* **84**, 585.
- Howarth, C. R., Foster, P. J. & Thrings, M. W. 1966 The effects of temperature on the extinction of radiation by soot particles. *Third Int. Heat Transfer Conf.* 5, p. 122.
- Janzen, J. 1979 The refractive index of colloidal carbon. *J. Colloidal Interface Sci.* **69**, 149.
- Janzen, J. 1980 Extinction of light by highly nonspherical strongly absorbing colloidal particles: spectrophotometric determination of volume distribution for carbon blacks. *Appl. Opt.* **19**, 2977.

- Jones, A. R. 1979 Electromagnetic wave scattering by assemblies of particles in the Rayleigh approximation. *Proc. R. Soc. Lond. A* **366**, 111.
- Ku, J. C. & Felske, J. D. 1986 Determination of refractive indices of Mie scatterers from Kramers–Krönig analysis of spectral extinction data. *J. opt. Soc. Am.* A **3**, 617.
- Lahaye, J. & Prado, G. 1981 Morphology and internal structure of soot and carbon blacks. *Particulate carbon* (ed. D. C. Siegla & G. W. Smith), p. 33. New York: Plenum Press.
- Latimer, P. 1972 Light scattering, data inversion and information theory. *J. Colloidal Interface Sci.* **39**, 497.
- Lee, S. C. & Tien, C. L. 1981 Optical constants of soot in hydrocarbon flames. In *Eighteenth Symp. (Int.) on Combustion*, p. 1159. The Combustion Institute.
- Menna, P. & D'Alessio, A. 1982 Light scattering and extinction coefficients for soot forming flames in the wavelength range from 200 to 600 nm. In *Nineteenth Symp. (Int.) on Combustion*, p. 1421. The Combustion Institute.
- Mie, G. 1908 Beiträge Zur Optiktrüber Medien speziell Kolloidaren Metallosunger. *Ann. Phys.* **25**, 377.
- Newton, R. G. 1966 *Scattering theory of waves and particles*. McGraw-Hill.
- Nussenzweig, H. M. 1972 *Causality of dispersion relations*. New York: Academic Press.
- Prado, G., Jagoda, J., Neoh, K. & Lahaye, J. 1981 A study of soot formation in premixed propane/oxygen flames by *in situ* optical techniques and sampling probes. *Eighteenth Symp. (Int.) on Combustion*, p. 1127. The Combustion Institute.
- Stull, V. R. & Plass, G. N. 1960 Emissivity of dispersed carbon particles. *J. opt. Soc. Am.* **50**, 121.
- Taft, E. A. & Philipp, H. R. 1965 Optical properties of graphite. *Phys. Rev. A* **138**, 197.
- Tomaselli, V. P., Rivera, R., Edewaard, D. C. & Möller, K. D. 1981 Infrared optical constants determined from reflection measurement. *Appl. Opt.* **20**, 3961.
- Weiner, A. M. & Harris, S. J. 1989 Optical detection of soot precursors. *Comb. Flame* **77**, 261.
- Wersborg, B. L., Howard, J. B. & Williams, G. C. 1973 Physical mechanisms in carbon formation in flames. In *Fourteenth Symp. (Int.) on Combustion*, p. 929. The Combustion Institute.

Received 12 December 1989; accepted 6 April 1990